Design and Verifications of an Autonomous Gain–Phase Sensor for Thick Beams

Y. P. Liu, Y. T. Huang, C. K. Lee, Jeremy W. J. Wu and Wendy W. H. Hsiao

Journal of Intelligent Material Systems and Structures 2005; 16; 955
DOI: 10.1177/1045389X05057521

Design and Verifications of an Autonomous Gain–Phase Sensor for Thick Beams

Y. P. Liu,[1] Y. T. Huang,[2] C. K. Lee,[1,2,*] Jeremy W. J. Wu[1] and Wendy W. H. Hsiao[3]

[1]*Department of Engineering Science and Ocean Engineering, National Taiwan University, Taipei, Taiwan*

[2]*Institute of Applied Mechanics, National Taiwan University, Taipei, Taiwan*

[3]*AdvanceWave Technologies, Inc., Taipei, Taiwan*

ABSTRACT: Both theoretical analysis and experimental verifications are performed on distributed sensors for Timoshenko beams. Development of a modal sensor for thick beams is hindered by the fact that it cannot be observed. It has been found that if we consider a modal sensor that neglects the shear strain effect in thick beams, we can develop an approximated modal sensor for thick beams. In addition, a previous concept is extended based on an *APROPOS* device (*A*utonomous *P*hase–gain *R*otational/linear *O*ptimum *P*iezoelectric *S*ensing) originally developed for thin beams to thick beams. Our successful results clearly show that autonomous gain and phase of thick-beam-based sensors and actuators are feasible.

Key Words: Timoshenko beam, thick beam, modal sensor, orthogonal condition, observability, *APROPOS* device.

INTRODUCTION

Modal Sensors (Lee and Moon, 1990; Lee, 1991) were initially developed to reduce the problem of spillover in structural feedback control. In traditional thin beam models, modal sensors can be attained by matching the surface electrode shape of a piezoelectric sensor to that of the strain distribution of the corresponding mode shape of the corresponding thin beam. However, for this model, it should be noted that an orthogonality condition needs to be embedded within the thin beam model to achieve the modal sensor. For a thick beam model, which is closer to real physical problems in MEMs or other structures possessing high natural frequency, the orthogonality condition is significantly different. This difference poses a very important limitation to the existence of corresponding modal sensors. This paper examines the relationship between the theory of Timoshenko beams and modal sensors. It will be shown first that due to the more complex orthogonal condition of thick beams, modal sensors based on thick beams suffer from an unobservable problem. In this study, we propose an approximated electrode concept to overcome this limitation.

STRUCTURE OF THICK BEAMS

Timoshenko beams, which are used to model thick beams, have three possible motions: bending, twisting, and stretching. In our mathematical model, we assumed the displacement u in the x-direction at an arbitrary distance z from the midplane to be:

$$u = u_0 + z\beta, \quad \beta = \gamma_{xz} - \frac{\partial w}{\partial x} \tag{1}$$

where u_0 is the stretching displacement on the neutral axes, w is the displacement along the z-axis, β is the rotation angle of the beam, and γ_{xz} is the shear strain (Figure 1(a)) along the z-direction on the x-plane. The shear strain induced on the cross section for thick beams is significant when compared to that of a thin beam case. Based on the Timoshenko beam theory, a thick beam of a rectangular cross section without any twisting or stretching ($u_0 = 0$) has an equation of motion as:

$$\frac{\partial Q}{\partial x} = \rho h \frac{\partial^2 w}{\partial t^2}, \quad \frac{\partial M}{\partial x} = Q + I\frac{\partial^2 \beta}{\partial t^2} \tag{2}$$

*Author to whom correspondence should be addressed.
E-mail: cklee@mems.iam.ntu.edu.tw

1045-389X/05/11/12 0955–8 $10.00/0 DOI: 10.1177/1045389X05057521

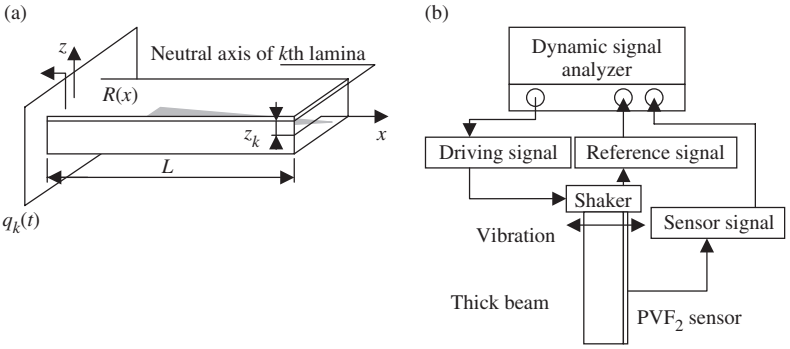

Figure 1. *Schematic of (a) thick beam model and (b) experimental set-up.*

where ρ, h, and $I = \rho h^3/12$ are density, thickness, and moment of inertia of the thick beam. In addition, M and Q are the moment and the transverse shear stress defined as:

$$M = D\frac{\partial \beta}{\partial x}, \quad Q = S\gamma_{xz} \tag{3}$$

where D and S are the flexural stiffness and the transverse shear stiffness. Substituting Equations (1) and (3) into Equation (2), we obtain the equation of motion:

$$S\left(\frac{\partial \beta}{\partial x} + \frac{\partial^2 w}{\partial x^2}\right) = \rho h \frac{\partial^2 w}{\partial t^2} \tag{4}$$

$$D\frac{\partial^2 \beta}{\partial x^2} = S\left(\beta + \frac{\partial w}{\partial x}\right) + I\frac{\partial^2 \beta}{\partial t^2} \tag{5}$$

Combining Equations (4) and (5), the equation of motion is simplified to:

$$D\frac{\partial^4 w}{\partial x^4} - \left[I + \frac{\rho h D}{S}\right]\frac{\partial^4 w}{\partial x^2 \partial t^2} + \frac{\rho h I}{S}\frac{\partial^4 w}{\partial t^4} + \rho h \frac{\partial^2 w}{\partial t^2} = 0 \tag{6}$$

The general solution of Equation (6) can be assumed to be as follows:

$$w(x, t) = \sum_{j=1}^{\infty} W_j(x) e^{i\omega_j t} \tag{7}$$

where i is $\sqrt{-1}$, ω_j represents the natural frequency of the thick beam, $W_j(x)$ is the mode shape of displacement, and subscript 'j' represents the jth mode. Combining Equations (6) and (7) leads to the mode shape:

$$W_j(x) = C_1 \cosh(\lambda_j x) + C_2 \cos(\lambda_j x) + C_3 \sinh(\mu_j x) + C_4 \sin(\mu_j x) \tag{8}$$

where λ_j and μ_j represent two different wave numbers of the evanescent wave and the propagating wave. These two wave numbers can be expressed as:

$$\lambda_j = \sqrt{\frac{\omega_j^2}{2D}\left(-\hat{I} + \sqrt{\hat{I}^2 + 4\hat{m}D}\right)}, \quad \mu_j = \sqrt{\frac{\omega_j^2}{2D}\left(\hat{I} + \sqrt{\hat{I}^2 + 4\hat{m}D}\right)} \tag{9}$$

where

$$\hat{I} = I + \frac{\rho h D}{S}, \qquad \hat{m} = \frac{\rho h}{\omega_j^2} - \frac{\rho h I}{S} \tag{10}$$

It is clear from Equation (6) that the additional term that appears in the Timoshenko beam model is contributed by the transverse shear strain effect. This added term induces two kinds of wave numbers for the mode shape of the Timoshenko beam. It can be shown that the mode shapes of displacement w in a Timoshenko beam are not orthogonal (Hu and Hwu, 1995). Since the Euler beam model, which is used to model thin beams satisfies the orthogonality condition in a Sturm–Liouville problem when considering homogeneous boundary conditions, the modes are orthogonal. This is the underlying reason why modal sensors can be easily implemented in an Euler beam (Lee, 1991).

The rotation angle β of a thin beam is different in a thick beam and can be traced to the presence of the shear strain. This is the reason why orthogonality is not present in a thick beam model. Looking at the rotation angle $\beta(x, t)$ equation, we obtain

$$\beta(x,t) = \sum_{j=1}^{\infty} B_j(x) e^{i\omega_j t} \tag{11}$$

where $B_j(x)$ is the mode shape of $\beta(x, t)$. We can then substitute Equations (7) and (11) into Equations (4) and (5) to obtain the relationship between $W_j(x)$ and $B_j(x)$:

$$\rho h \omega_j^2 W_j(x) = -S(B_j'(x) + W_j''(x)) \tag{12}$$

$$I\omega_j^2 B_j(x) = -(DB_j''(x) - SB_j(x) - SW_j''(x)) \qquad (13)$$

By combining and simplifying Equations (12) and (13), and incorporating the four boundary conditions, i.e., $w=0$, $\beta=0$, $Q=0$, and $M=0$; the orthogonal relationship composed of $W_j(x)$ and $B_j(x)$ becomes:

$$(\omega_i^2 - \omega_j^2)\int_0^L (\rho h W_i W_j + IB_i B_j)\,\mathrm{d}x = 0 \qquad (14)$$

Substituting Equations (12) and (13) and the boundary conditions into Equation (14) and then performing integration by parts, another orthogonal relationship can be obtained where:

$$\int_0^L \left[S(B_i + W_i')(B_j + W_j') + DB_i' B_j'\right]\mathrm{d}x = \delta_{ij} \qquad (15)$$

where $\delta_{ij} = 1$ if $i=j$ and $\delta_{ij} = 0$ if $i \neq j$. Equations (14) and (15) indicate that the orthogonal relationship of the thick beam can be identified if the rotation angle $\beta(x, t)$ is taken into consideration.

SENSOR EQUATION OF PIEZOELECTRIC LAMINATES

Owing to its flexibility, PVF_2 was used as the piezoelectric material to construct the sensors. It is known that PVF_2 possesses *mm*2 symmetry and thus only five different piezoelectric constants are needed. We mounted the piezoelectric laminate on top of a composite thick beam to sense the bending motion. By taking a plane stress approximation, the closed-circuit charge signal $q_k(t)$ generated from the surface electrode of the kth layer piezoelectric lamina can be expressed as:

$$q_k(t) = z_k e_{31} \iint_{\bar{S}} \frac{\partial \beta}{\partial x}\mathrm{d}x\,\mathrm{d}y \qquad (16)$$

where e_{31}, e_{32}, and e_{36} are the piezoelectric stress/charge constants, z the distance between the neutral axis of the thick beam and the middle of the kth lamina, and $\overline{S}$ the area of the surface electrode of the piezoelectric lamina.

Since the deformation in the y-direction is very small, i.e., $w = w(x, t)$, the surface electrode distribution in the y-direction can be regarded as the weighting factor to arrive at the orthogonality condition (Lee, 1991; Lee and Moon, 1990). Assuming that $R(x)$ is the shape of the effective surface electrode, Equation (16) can be rewritten as:

$$q_k(t) = z_k e_{31} \int_0^L R(x)\frac{\partial \beta}{\partial x}\mathrm{d}x \qquad (17)$$

It is known that a piezoelectric lamina can also be pasted onto the lateral side of a thick beam. However, since there are two dependent directions of the lateral surface electrode, it is difficult to design an effective surface electrode shape without introducing unwanted effects.

As Equations (11) and (17) show that the piezoelectric lamina can sense $B_j'(x)$ only, it cannot lead us directly to the orthogonality condition as depicted in Equation (15). That is, modal sensors of a Timoshenko beam suffers from an unobservable condition.

APPROXIMATED THICK-BEAM MODAL FILTERS

As the mode shapes of thick beams are not orthogonal, an approximation must be used if we are to approach a modal sensor effect. More specifically, to develop a design that can be adopted to use an approximated thick-beam modal filter, we must use a concept similar to that used with thin-beam modal sensors. The thin beam orthogonality condition is thus:

$$\int_0^L W_i''\, W_j''\,\mathrm{d}x = \delta_{ij} \qquad (18)$$

Substituting the second part of Equation (1) into Equation (17), the thick beam sensor equation can be described by displacement w:

$$q_k(t) = z_k e_{31} \int_0^L R(x)\left(\frac{\partial \gamma_{xz}}{\partial x} - \frac{\partial^2 w}{\partial x^2}\right)\mathrm{d}x \qquad (19)$$

Comparing Equations (18) and (19), the shear strain effect of the thick beam sensor equation can be neglected so that we can develop an approximated modal sensor. However, it should be noted that the approximation was done only by neglecting the shear strain effect in the sensor equation since the two wave number conditions of the thick beam are retained. The electrode shape of modal filters chosen is thus:

$$R(x) = W_j''(x) \qquad (20)$$

APROPOS DEVICE OF THICK BEAMS

Unlike the orthogonality requirement associated with modal sensors, an *APROPOS* (*A*utonomous *P*hase-gain *R*otational/linear *O*ptimum *P*iezoelectric *S*ensing) device (Hsu and Lee, 2002) concept was developed by utilizing a dispersion relationship of the sensor structure, i.e., no orthogonality condition is needed. Thus,

the solution of Equation (8) can be broken down as follows:

$$w(x,t) = (w_{le}e^{\lambda x} + w_{re}e^{-\lambda x} + w_{lp}e^{i\mu x} + w_{rp}e^{-i\mu x})e^{i\omega t} \tag{21}$$

where subscript 'lp' represents the leftward propagating wave mode, 're' represents the rightward emanating evanescent mode, 'le' represents the leftward emanating evanescent mode, and 'rp' represents the rightward propagating wave mode. The *APROPOS* device concept can be used to design different kinds of autonomous filters for the transfer function at the targeted origin (Hsu and Lee, 2002). To examine the possibility of using an *APROPOS* device for thick beam vibration control, a low-pass spatial filter with its corner frequency designed to filter out all resonance frequencies except the first frequency was designed. Substituting Equation (4) into Equation (17) and extending the finite domain into an infinite domain, the new sensor equation for a thick beam *APROPOS* device can be obtained where:

$$q_k(t) = -z_k e_{31} \int_{-\infty}^{\infty} R(x)\left(\frac{\partial^2 w}{\partial x^2} + \frac{\rho h}{S}\frac{\partial^2 w}{\partial t^2}\right) \mathrm{d}x \tag{22}$$

Combining Equations (21) and (22), and adopting the symmetry condition yields:

$$\begin{aligned} q_k(\mu,\lambda) = -z_k e_{31}\Bigg[&\left(\frac{\rho h\omega^2}{S} - \mu^2\right)(w_{lp} + w_{rp}) \\ &\times \int_{-\infty}^{\infty} R(x)e^{-j\mu x}\,\mathrm{d}x + \left(\frac{\rho h\omega^2}{S} + \lambda^2\right) \\ &\times (w_{le} + w_{re})\int_{-\infty}^{\infty} R(x)e^{-\lambda x}\,\mathrm{d}x\Bigg] \end{aligned} \tag{23}$$

To null the surface electrode at the boundary similar to that of the typical method taken in a thin beam approach, the sine and cosine functions were used as their two-sided Laplace transformations lead to delta functions in an s-domain. Taking the sine and the cosine functions to the effective surface electrode as designed not only made the finite structure extend into an infinite domain, but it also does not change the effect of the surface electrode. Choosing effective surface electrode $R(x) = e^{-a|x|} - b\sin(cx)$ with a as a corner wave number and b, c as constants that can make the weighting function of boundary approach zero, yields a desired autonomous gain–phase low-pass filter with respect to the targeted origin:

$$\begin{aligned} q_k(\mu,\lambda) = -z_k e_{31}\Bigg[&\left(\frac{\rho h\omega^2}{S} - \mu^2\right)(w_{lp} + w_{rp})\frac{2\mu}{\alpha^2 - \mu^2} \\ &+ \left(\frac{\rho h\omega^2}{S} + \lambda^2\right)(w_{le} + w_{re})\frac{2\lambda}{\alpha^2 + \lambda^2}\Bigg] \end{aligned} \tag{24}$$

It is clear from Equations (23) and (24) that thick-beam *APROPOS* devices have additional terms to adjust the frequency responses of the targeted origin. However, the dispersion is far more complex in a thick beam than in a thin beam. By setting a targeted origin at the free end of a thin beam, we can produce a −20 dB/decade low-pass filter in a frequency domain (Hsu and Lee, 2002). On the other hand, setting the targeted origin at the fixed end of a thin beam will produce a −10 dB/decade low-pass filter in a frequency domain (Hsu and Lee, 2002). In a thick beam structure, the two different wave numbers μ and λ are approximately the same at low frequencies. It can be seen that an *APPROPOS* device in a thick beam will produce an approximated −10 dB/decade low-pass filter in a frequency domain on the targeted origin under the condition when the targeted origin is set at the fixed end.

EXPERIMENTAL SETUP

Aluminum beams with three different thicknesses (1, 2, and 5 mm) were chosen as the specimens, all of which were 160 mm long by 22.75 mm wide. The Young's modulus of aluminum was 70 GPa. The measured density was 2720 kg/m^3 and the Poisson's ratio was assumed to be 0.303. Although, theoretical analysis was performed for all the three specimens, only the 1 and 2 mm thick aluminum beams were tested. The experimental setup is shown in Figure 1(b).

For a cantilever beam case, four boundary conditions can be obtained:

$$\begin{aligned} w|_{x=0} &= 0, \qquad \beta_x\big|_{x=0} = 0, \\ S\left(\beta + \frac{\partial w}{\partial x}\right)|_{x=L} &= 0, \qquad D\frac{\partial \beta}{\partial x}\bigg|_{x=L} = 0 \end{aligned} \tag{25}$$

where L is the length of the beam. Equations (6) and (11) lead to a boundary value problem, where the natural frequency and the displacement mode shapes of the thick beams obtained are:

Natural frequency equation

$$\begin{aligned} &2 + \left(N - \frac{1}{N}\right)\sin(\mu_j L)\sinh(\mu_j L) \\ &\quad + \left(\Lambda N + \frac{1}{\Lambda N}\right)\cos(\lambda_j L)\cosh(\lambda_j L) = 0 \end{aligned} \tag{26}$$

where

$$\Lambda = \frac{\lambda_j + (\rho h\omega_j^2/G\lambda_j)}{\mu_j + (\rho h\omega_j^2/G\mu_j)}, \quad N = \frac{\lambda_j}{\mu_j} \tag{27}$$

Mode shape

$$W_j(x) = \cosh(\lambda_j x) - \cos(\mu_j x) - \left(\frac{1}{\Lambda}\sinh(\lambda_j x) - \sin(\mu_j x)\right) \times \left(\frac{\cos(\mu_j L) + \Lambda N \cosh(\lambda_j L)}{\sin(\mu_j L) + N \sinh(\lambda_j L)}\right) \quad (28)$$

Table 1. Natural frequency of the three beam specimens.

	1st mode		2nd mode	
Thickness (mm)	Thin beam (Hz)	Thick beam (Hz)	Thin beam (Hz)	Thick beam (Hz)
5	165.911	165.790	1039.750	1034.800
2	65.225	65.218	408.763	408.433
1	31.769	31.768	199.097	199.056

By using the theorem mentioned above, the natural resonant frequency can be calculated (Table 1).

Modal Sensors for Thick Beam Structures

The electrode shape of modal filters chosen were:

$$R(x) = W_1''(x) = R_1\cosh(\mu_1 x) + R_2\sinh(\mu_1 x) + R_3\cos(\lambda_1 x) + R_4\sin(\lambda_1 x) \quad (29)$$

Considering the natural resonant frequency of the thick beam listed in Table 1 as well as the boundary conditions, the design parameters used to design the modal sensors can be computed and summarized in Table 2.

A charge amplifier was used to amplify the charge signal from the PVF_2. A dynamic signal analyzer, SR780 (Stanford Research Systems, Inc., 1996) from Stanford Research, was used to measure the transfer

Table 2. Design parameters for approximated thick-beam modal sensors.

Thickness (mm)	λ_1	μ_1	R_1	R_2	R_3	R_4
1	0.0117191	0.0117194	5.68738	4.99864	5.68762	4.99908
2	0.0117182	0.0117192	5.68700	4.99812	5.68800	4.99989
5	0.0117119	0.0117184	5.68437	4.99450	5.69063	5.00549

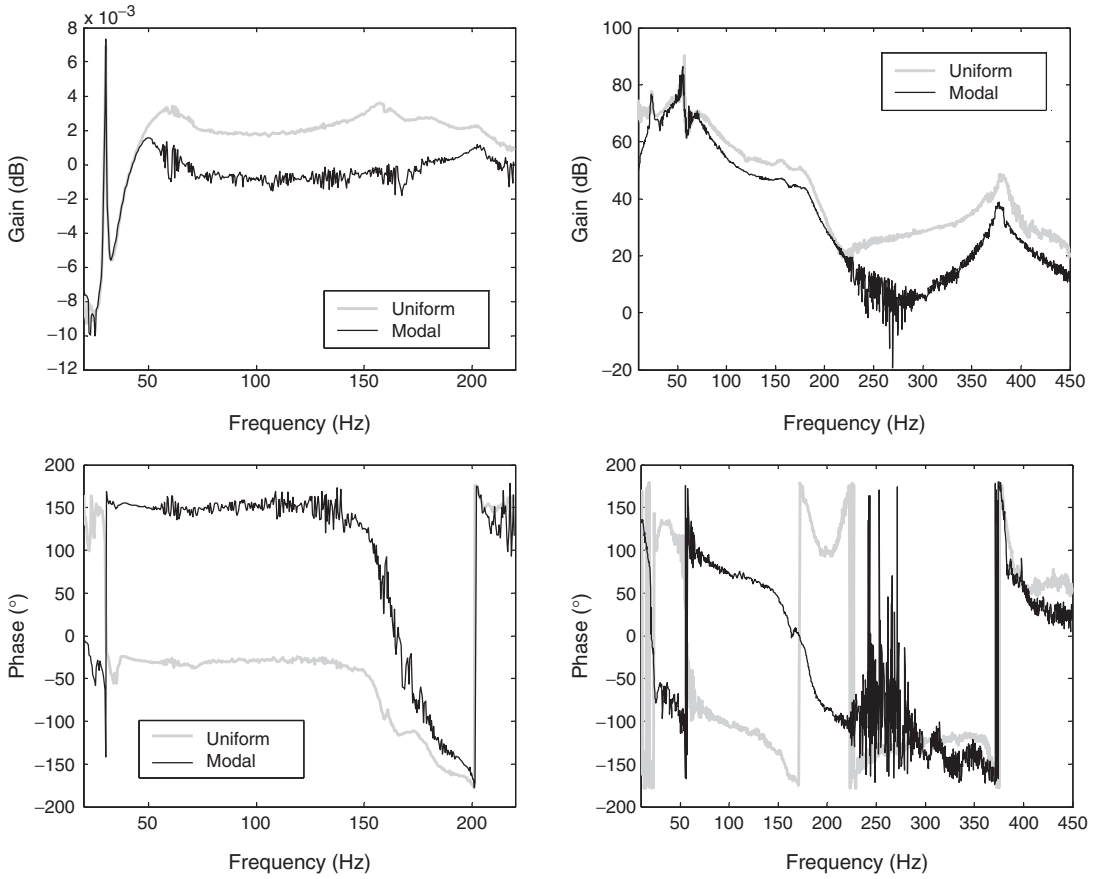

Figure 2. *Comparisons of the frequency responses of uniform and modal sensors for 1 mm (left) and 2 mm (right) aluminum beams.*

function of the thick-beam-based modal sensor. Owing to the limitations of setting up an experimental setup, a photonic sensor (MTI 2000, 1991) was used to measure the shaker displacement when the 1 mm thick aluminum beam was mounted. However, when the accelerometer was used to measure the shaker acceleration of a 2 mm thick aluminum beam, the shaker displacement was too small in the frequency range of interest. To compare the data in an equivalent manner, the transfer function measured for the 1 mm thick aluminum beam was converted by performing pseudo differentiation twice to become acceleration (e.g., multiplying displacement by the product of -1 and the square of the angular frequency $-\omega_j^2$ which leads to acceleration in a frequency domain).

The frequency responses of the 1 mm aluminum beam measured are shown in Figure 2. Two piezoelectric sensors, one uniform and the other modal, were mounted on the top and the bottom surfaces of the aluminum beam to verify the effect of the approximated modal filter. It is clear from the data shown in Figure 2 that the uniform sensor and the modal sensor have the same amplitude at the first natural frequency. In addition, the measured resonance matched well with the theoretical predictions shown in Table 1. However, the filtering effect was quite prominent in the modal sensor when considering the second resonant frequency. It should be noted that no phase change is present when gain is tailored. This autonomous gain and phase tailoring matches what was predicted using the *APROPOS* device theory.

The frequency responses of the 2 mm aluminum beam are shown in Figure 2. The accelerometer was used to measure the shaker acceleration, which was used as the reference signal. The measured resonance matches well with the theoretical predictions, as shown in Table 1. It is clear from Figure 2 that the amplitude for the modal electrode is lower than that for the uniform electrode at the second resonant frequency. More specifically, the approximated modal sensor does

Table 3. Design parameters for thick-beam APROPOS devices.

Thickness (mm)	*a*	*b*	*c*	Designed corner frequency (Hz)
1	0.0131501	0.121966	0.0098175	40
2	0.0129790	0.125351	0.0098175	80
5	0.0122069	0.141834	0.0098175	180

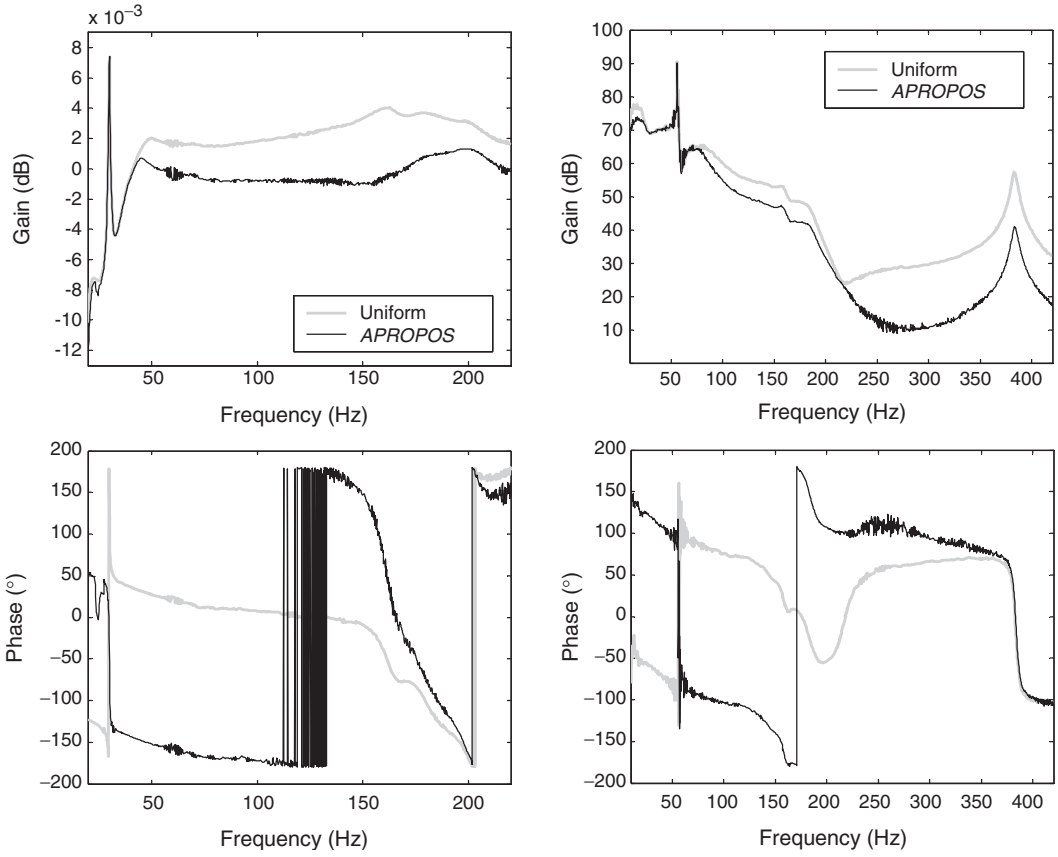

Figure 3. *Comparisons of the frequency responses of the uniform sensor and APROPOS device sensor for the 1 mm (left) and 2 mm (right) aluminum beam.*

possess a mode filtering effect. It is also clear that gain tailoring was not associated with a phase change in the beam case. This set of experimental data clearly dictates that thick-beam modal sensors can be properly approximated by neglecting the shear strain effect.

APROPOS Device for Thick Beam Structures

According to the principle of an *APROPOS* device, a no-phase delay low-pass filter can be created for a thick beam. We set the targeted origin at a fixed end and the effective surface electrode shape can be chosen as:

$$R(x) = e^{-a|x|} - b\sin(cx) \tag{30}$$

It is easy to set the parameter 'a' to the designed corner frequency and set the parameters 'b' and 'c' to the boundary conditions. The solutions are shown in Table 3.

Similar to the testing of the modal sensor case, the same experimental conditions were applied to verify the performance of the thick-beam *APROPOS* device sensors. The result for the 1 mm thick beam (Figure 3) shows that the gain begins to drop for frequencies higher than 40 Hz. This phenomenon matches the theoretical design of the *APROPOS* device since the autonomous low-pass no-phase delay filter was set to have a 40 Hz corner frequency. The same kind of gain tailoring behavior was found on the 2 mm thick aluminum beam even though the corner frequency of the 2 mm thick beam was set at 80 Hz.

To observe the effect of the *APROPOS* device more directly, a new experimental setup was designed. An *APROPOS* device-based sensor and an uniform sensor were mounted on both sides of a thick beam (Figure 4). By dividing the signals from the *APROPOS* device and the uniform sensor in real time leads us to a corner frequency effect. The data shown in Figure 5 clearly demonstrates that an *APPROPOS* device concept is equally valid for thin beams as well as thick beams.

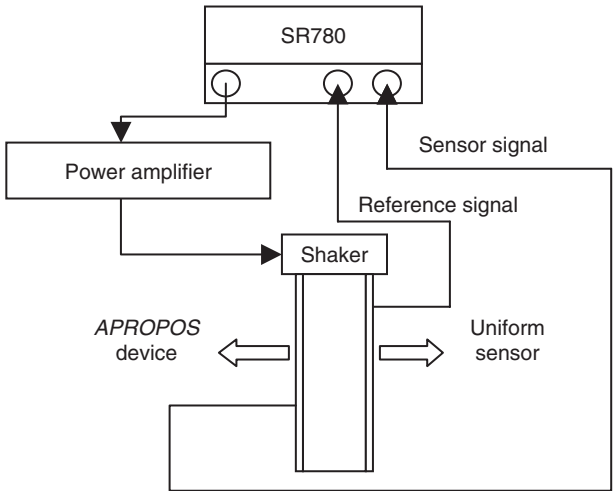

Figure 4. *Experimental setup for corner frequency verifications.*

CONCLUSIONS

In our study, we developed an orthogonality condition for thick beams since an unobservable condition hinders the implementation of modal sensors for thick beams. We found that modal sensors developed by neglecting a shear strain effect can be used to sufficiently approximate modal sensors for thick beams. A theoretical model of a thick beam-based *APROPOS* device was developed. Results show that the tailored frequency response of our designed autonomous gain and phase low-pass filters matches the theoretical predictions.

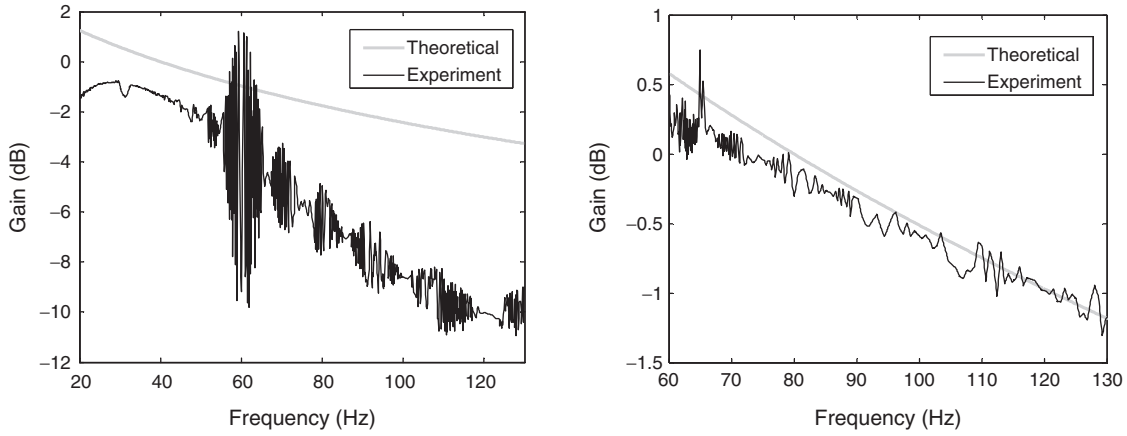

Figure 5. *Corner frequency measurement of 1 mm (left) and 2 mm (right) for APROPOS device-based sensor.*

ACKNOWLEDGMENTS

The authors are grateful to Measurement Specialties, Sensor Products Division (MSI) for continuously providing us with all the PVF_2 films used in fabricating the piezoelectric devices discussed in the research work. The funding from National Science Council, Taiwan under Project NSC 93-2622-E-002-003 is gratefully acknowledged.

REFERENCES

Hu, J.S. and Hwu, C.B. October 1995. "Free Vibration of Delaminated Composite Sandwich Beams," *AIAA Journal*, 33(9):1–8.

Hsu, Y.H. and Lee, C.K. June 2002. "Targeted Origin Placement for Autonomous Gain-Phase Tailoring of Piezoelectric Sensors," *Smart Materials and Structures*, 11(3): 444–458.

Lee, C.K. 1991. "Piezoelectric Laminates: Theory and Experiments for Distributed Sensors and Actuators," In: Tzou, H.S. and Anderson, G.L. (eds), *Intelligent Structural Systems*, pp. 75–167, Kluwer Academic Publishers, Netherlands.

Lee, C.K. and Moon, F.C. June 1990. "Modal Sensors/Actuators," *Journal of Applied Mechanics–Transactions of the ASME*, 57(2):434–441.

MTI 2000, March 1991. *Fotonic Sensor Instruction Manual*, MTI Instruments, Inc., Washington Avenue Extension, Albany, NY 12205, USA.

Stanford Research Systems, Inc. July 1996. *Operating Manual and Programming Reference: Modal SR780 Network Signal Analyzer*, Stanford Research Systems, Inc., 1290-D Reamwood Avenue, Sunnyvale, CA 94089, USA.